27th ABCM International Congress of Mechanical Engineering
December 04-08, 2023, Florianópolis-SC, Brazil

# COB-2023-1389
# USING AN INVERSE METHOD BASED ON DEEP LEARNING TO OBTAIN SHEAR PARAMETERS TO OPTIMIZE A SHEAR-DISPLACEMENT FINITE ELEMENT SOLUTION

**Luana Claudia Bertoncello**
**Francisco Augusto Aparecido Gomes**
**Robson Trentin**
**Paulo Rogério Novak**
*Federal University of Technology - Paraná, Pato Branco- PR, Brasil*
luanabertoncello@alunos.utfpr.edu.br, franciscogomes@utfpr.edu.br, robsontrentin@utfpr.edu.br, novak@utfpr.edu.br

***Abstract.*** *The application of computational simulation using finite element methods has been intensified to solve engineering problems. The technique adopted in this work is known as a solution based on an inverse problem. This technique is based on the optimization of certain input parameters, which will be used to minimize errors in the main physical solution. The objective of this work is to develop a computer simulation using the finite element method in conjunction with an algorithm based on deep learning to minimize solution errors. The application of deep learning in engineering has been growing in recent years, due to its ability to solve and minimize errors in complex problems. Through the use of artificial neurons, the main feature of the neural network is to simulate the functioning of human neurons that are interconnected by an artificial synapse. The numerical study will be based on the direct pullout test of a semi-smooth steel bar immersed in a concrete specimen, whose experimental data will be the input data of the neural network. In this case, input parameters such as shear stress and adhesion will be optimized from the neural network, in which shear will characterize concrete failure due to steel bar slippage. A validation of the numerical methodology will be presented to analyze the efficiency of the optimization method in relation to the accuracy of the physical solution, considering values of the bond stress between the steel bar and concrete (shear) and the sliding of the steel bar in relation to the concrete.*

***Keywords:*** *optimization, inverse solution, finite element methods, neural network.*

## 1. INTRODUCTION

It is possible to obtain the interaction between steel and concrete through friction, mechanical means, and adherence. In the case of bonding, this interaction is characterized by bonding stress and sliding of the bar on concrete. Due to its relevance for structural performance, this steel-concrete relationship has been explored by other authors over the years, such as Almeida Filho (2006), Simplício (2008), Tojal (2011), Hong and Park (2012), Rosales (2016), among other literature.

While the use of software and tools based on finite element methods was progressively conquering more space in various fields of engineering, such as in simulations to predict behavior, optimization of solutions, and more detailed analyzes, among others, the use and the evolution of this set between computational system and FEM. Focusing on the improvement and accuracy of numerical models, the application of FEM requires some information such as input data, law of behavior, geometry, and meshes. (Naranjo-Pérez et al., 2020)

The main concept involved in this method is to discretize a complex problem working with small sets to be analyzed. Understanding a certain level of maturity, the FEM enables the solution of problems through two types of analysis, direct or inverse. The direct analysis assumes that the boundary condition and initial conditions are known and informed as input data to perform the simulation. While the inverse analysis uses data referring to the end of a process in order to find the best conditions to give rise to the start of the simulation. (Stahlschmidt, 2010).

Solution optimization based on inverse problems can be studied as a response to elastic excitations (dynamic or static displacements), thermal, electrical, or other flows, as discussed by Rus and Gallego (2002). This study has as its main objective to identify the parameters of existing research on the behavior of an experimental problem of direct pullout, related to shear stress and, applying the optimization based on neural network, employing algorithms and simulations by FEM, elucidating the inverse problem involving steel-concrete interaction.

## 2. MATERIALS AND METHODS

Aiming to obtain the numerical solution of the physical problem with the lowest error rate, the reading of the experimental data will be performed and through the objective function the deviation between the experimental and numerical results will be calculated. To obtain results, a routine with parameters, genetic algorithms, objective function, obtained results and expected results for convergence must be monitored.

## 2.1 **Parameter identification**

From a convergence problem it is possible to identify the parameters for the optimization, as it is based on which simulation variables make it possible to minimize the gap between the experimental and numerical curves. The identification of parameters consists of an experimental test, the mathematical model, characterization of the materials, and boundary conditions. In this work, the mathematical model will be based on the finite element method with the study of the inverse problem from an objective function. (Kleinermann and Ponthot, 2003)

As previously mentioned, knowledge of the geometry of experimental samples is also of paramount importance. In this study, the samples have an initial cylindrical geometric configuration with the following dimensions: concrete specimen with ø 100mm and height of 100mm and semi-smooth steel bar with ø10mm, as shown in figure 1.

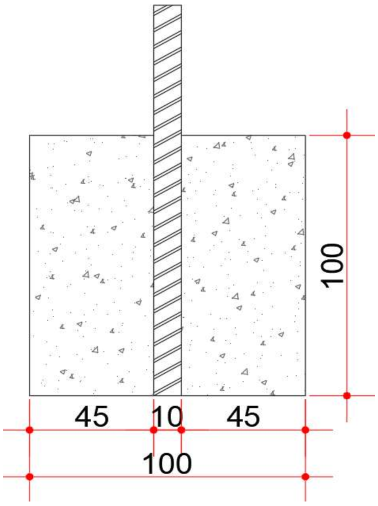


Figure 1. Representation of the considered model. (Own authorship, 2023)

For the simulation in the APDL language, the axisymmetric pattern in two directions (2D) was adopted, since the sample geometry is symmetrical and the efforts are uniform. Modeling the 2D solid structure in the mesh simulation, the 4-node PLANE 182 was used as an element for plane stress and strain, due to its plasticity, stress stiffness, large deflection, and large deformation capabilities. (ANSYS, 2023)

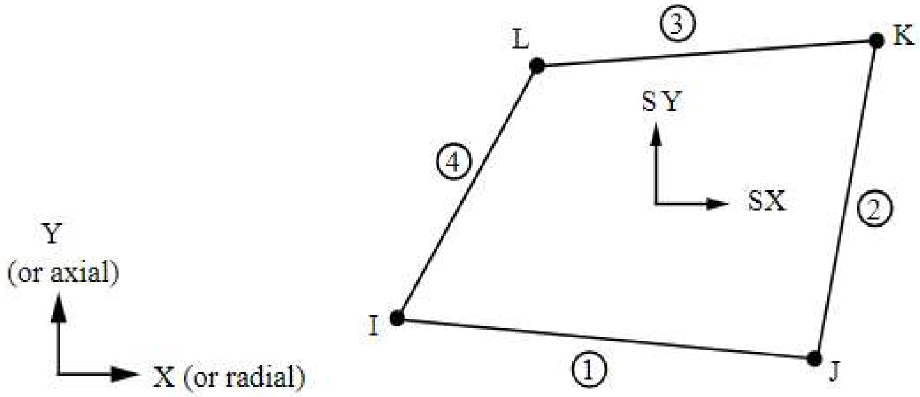


Figure 2. PLANE182 Stress Output. (ANSYS, 2023)

To reduce the discrepancy between the curves as mentioned at the beginning of this item is directed to the objective function, this authorization was also used by other authors, such as Stahlschmidt (2010), and Kleinermann and Ponthot (2003). In figure 3 it is possible to understand the arrangements of the variables, where $Fi\ EXP$ is the ordinate of the ith experimental point, $Fi\ MEF$ is the ordinate of the ith experimental point numeric obtained by FEM.

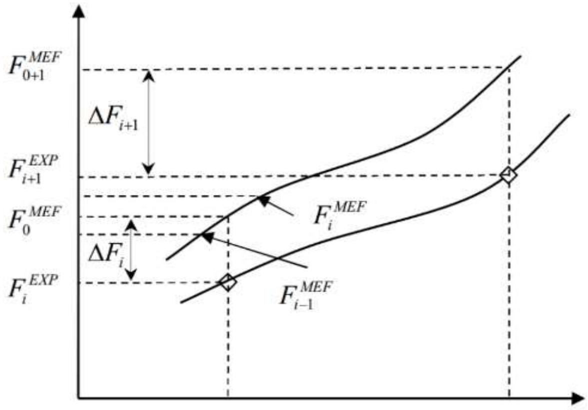


Figure 3. Experimental-FEM simulation. (Trentin, 2009)

## 2.2 Deep Learning

Deep learning is a subfield of computer science whose main objective is to train machines to perform human tasks. This training is composed of an algorithm that not only learns the data but also features perception, decision-making, and problem-solving. Being developed similarly to the human neural system, it works with integrated artificial neural networks of multilayers and neurons to store data. In figure 4 we can understand the temporal technological evolution and the subareas of artificial intelligence. (Kayabekir et al., 2023)

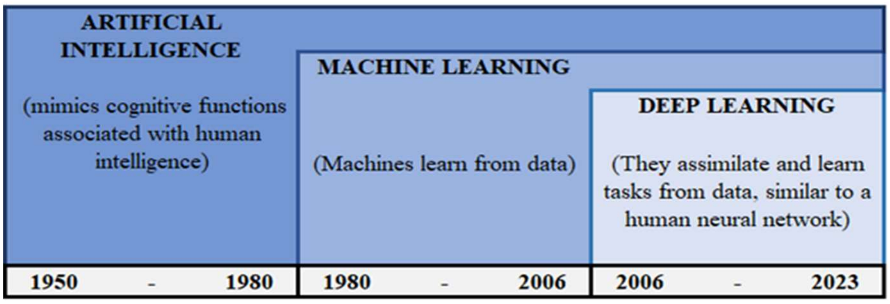


Figure 4. Artificial Intelligence, Machine Learning, and Deep Learning chronological order. (Kayabekir et al., 2023)

According to Kayabekir et al. (2023) the use of deep learning has brought great interest in engineering due to its structure, fast processors and ease of implementation. The authors mention that by using deep learning in engineering sectors it is possible to obtain data and solutions to complex problems, such as displacement, vibrations in buildings, energy flow, and damage.

Deep learning works with computational neurons, which have the function of learning and transmitting information. Not every network follows the same pattern of computational neuron numbers, they can vary both the number of layers and the number of neurons in each layer. The artificial neuron is also capable of receiving more than one input signal, but it can only have a single output signal. In the synapse, they are where the weights of the layers, known as $w_n$, are stored. After completing the first iteration, in case of non-convergence in the output, the layers receive a new weight and start to represent new values for the new data processing, as illustrated in figure 5. (Haykin, 2008)

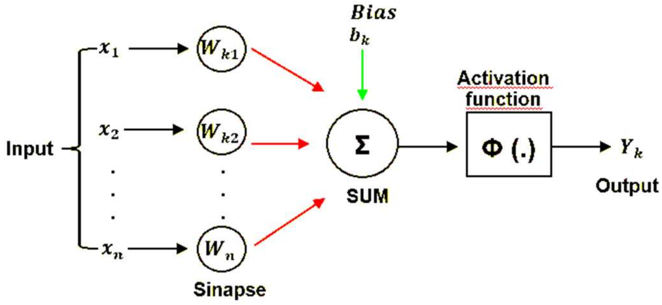


Figure 5. Deep Learning structure. (Haykin, 2008)

Describing the process of this work the input is related to the experimental input data, the synapse represents the simulation elaborated by the APDL, while in the Bias and in the activation of the function the learning process occurs to optimize and compare if there was convergence.

2.3 **Numerical method**

Based on the mechanical parameters obtained from the experimental data, the numerical implementation was through Drucker-Prager in order to analyze their behavior, according to Eq (1). Focusing on the adhesion stress of the slide of the bar on the concrete specimen.

$$f(\sigma, \sigma_Y) = \sigma_e + \alpha \frac{1}{3} tr(\sigma) - \sigma_y, \tag{1}$$

Where σ_Y corresponds to uniaxial yield stress, σ_e equivalent stress, and α corresponds to pressure sensitivity. Still regarding α, it is a function of the internal friction angle following Equation (2).

$$\alpha = \frac{6 sin\, \emptyset}{\sqrt{3}(3 - sin\, \emptyset)}, \tag{2}$$

In Eq (3), the numerical model of the objective function used to reduce the discrepancy between the curves was described. This was adopted according to the literature review and the similarity of this procedure with that of other authors, as mentioned in the identification parameters item.

$$f(obj) = \sqrt{\frac{1}{n} \sum_{i=1}^{n} \cdot \left(\frac{Fi^{FEM}(bj) - Fi^{EXP}}{Fi^{exp}}\right)^2}, \tag{3}$$

Where $f(obj)$ corresponds to the objective function, $n$ represents the number of experimental points, $Fi\ EXP$ is the ordinate of the ith experimental point, $Fi$ FEM is the ordinate of the ith experimental point numeric obtained by FEM.

2.4 **Results**

The experimental data were obtained from the article by the authors Luvison et al. (2022), considering only the result referring to the semi-flat steel bar BSL. In figure 6, it is possible to visualize the curve of adhesion stresses by sliding, while in table 1 it presents with greater clarity and precision the results obtained by the authors.

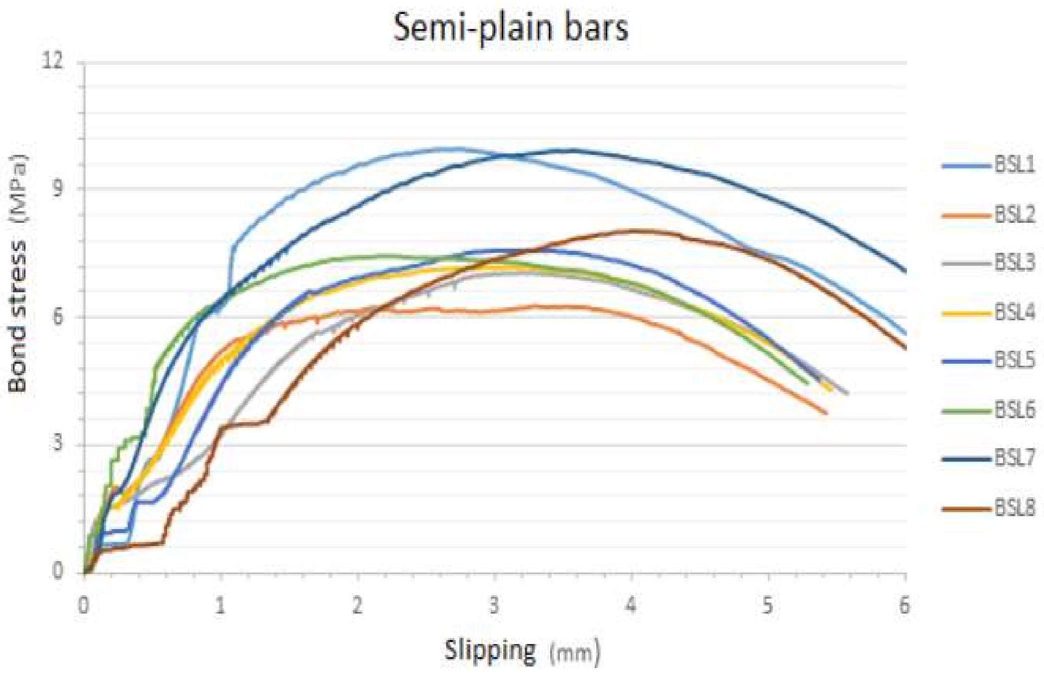


Figure 6. Graph of bond stress by slipping specimens with semi-plain bars. (Luvison et al., 2022)

Table 1. Stresses and slipping for specimens with semi-plain bars - (Luvison et al.,2022)

| Specimen identification | Maximum stress (MPa) | Final stress (MPa) | Maximum slipping (mm) |
|---|---|---|---|
| BSL1(1) | 9,96 | 5,07 | 2,74 |
| BSL2(1) | 6,37 | 3,81 | 3,30 |
| BSL3(1) | 7,04 | 4,22 | 3,20 |
| BSL4(1) | 7,19 | 4,30 | 3,08 |
| BSL5(1) | 7,58 | 4,54 | 3,24 |
| BSL6(1) | 7,45 | 4,45 | 2,20 |
| BSL7(1) | 9,92 | 5,87 | 3,57 |
| BSL8(1) | 8,03 | 4,80 | 4,02 |
| Mean | 7,94 | 4,63 | 3,17 |
| DP | 1,32 | 0,63 | 0,54 |
| CV (%) | 16,64 | 13,52 | 17,03 |

(1) BSL stands for semi-plain bars.

The experimental results regarding the maximum resistance for semi-smooth bars reached approximately 12kN, the authors mention that this response varies according to the type of bar used in the test, that is, for smooth bars the maximum resistance was lower, due to the lack of roughness in the material, while in ribbed bars the resistance was higher due to the higher degree of roughness of the bars.

To validate the method, the aforementioned authors developed a numerical model aiming to find the numerical resistance curve sliding the semi-smooth bar. For numerical simulation, different tensile loads were applied, following the values: 2 kN, 4 kN, 6 kN, 8 kN, 10 kN, 12 kN. Varying the values every 2 kN until reaching the maximum resistance reached by the experimental test.

For the simulations, the Drucker-Prager method was used in order to analyze the compressive stress levels and Von Mises for ductile materials. Regarding the boundary condition, restrictions were applied on the y and z axes, respectively, horizontal and vertical. To apply the displacement, node 100000 was adopted, located at the top of element 1 (BSL bar), to join all nodes in order to simplify the reading of the force through a single node, as shown in figure 7.

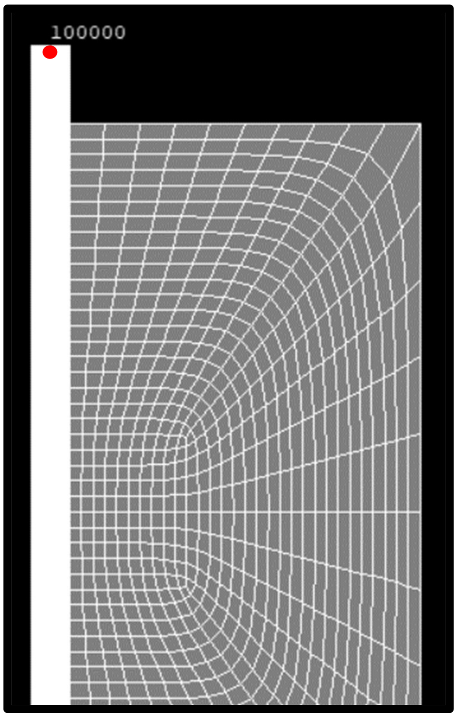


Figure 7. Node 10000. (Own authorship, 2023)

Figure 8 and 9 are showing the mesh used. It is worth mentioning that the mesh is extremely important for work in this segment since it defines the contact between the surfaces and can directly interfere with the desired results. There is a specific circumstance in relation to her choice that generates some consideration, the level of refinement of the mesh.

Because the more you refine this element, the greater the accuracy, but the greater the simulation time and computational cost. For this reason, we opted to refine the mesh on the semi-smooth bar and in regions where there is contact, and for other locations, a coarser texture was chosen.

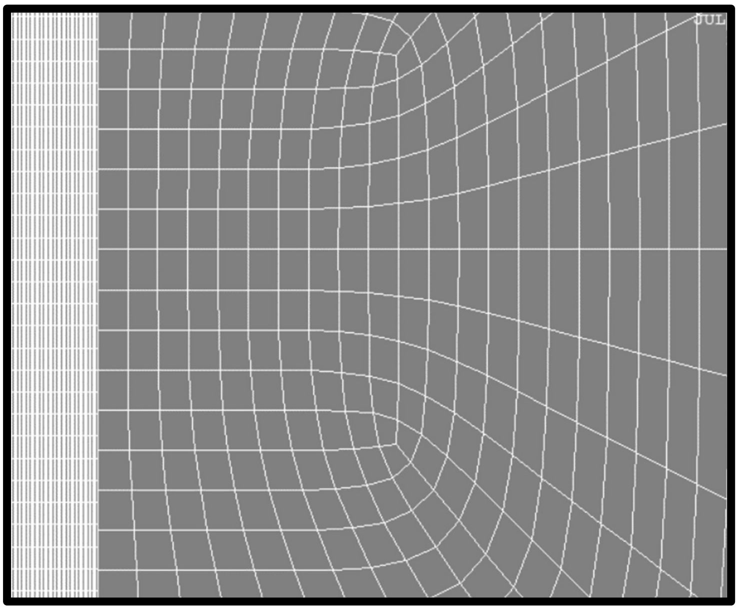


Figure 8. Approximate model of the axisymmetric mesh. (Own authorship, 2023)

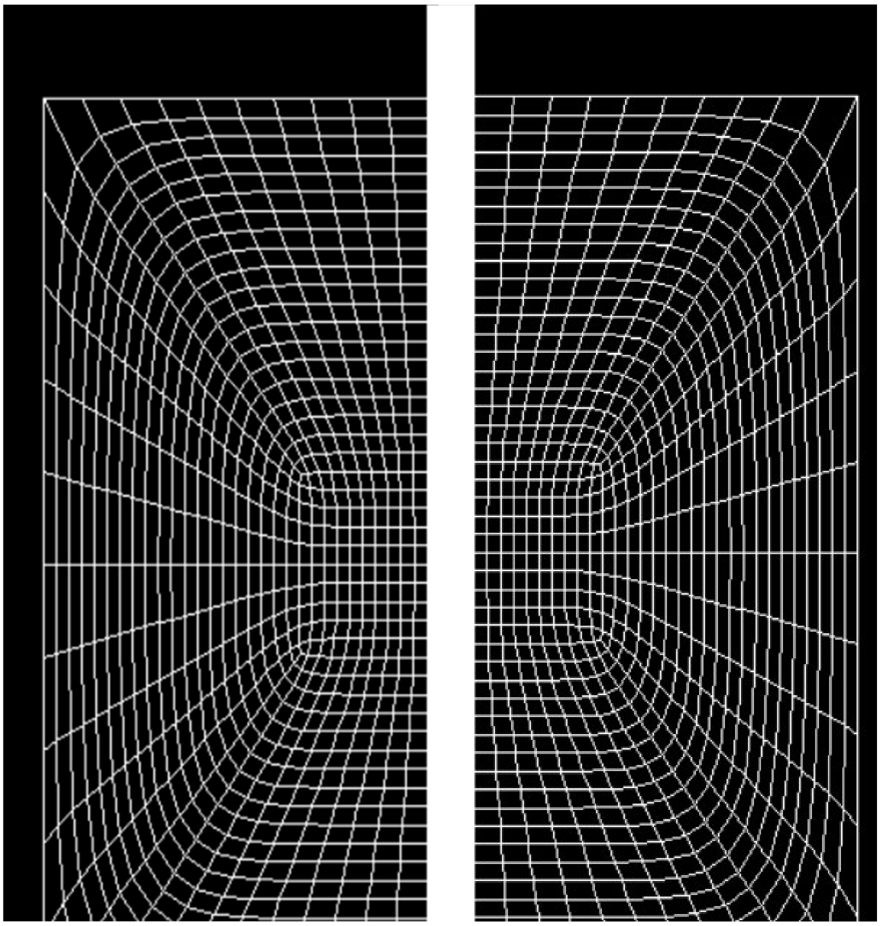

Figure 9. Mesh geometry. (Own authorship, 2023)

Considering that the geometry of the samples is symmetrical and the efforts applied are uniform, in this work the solution was through the hypothesis of axial symmetry, therefore the execution of the simulation was only in 2D (two dimensions).

From the presented literature and knowing the experimental data of the BSL bar, considering displacement, constitutive model, and coefficient of friction. Figure 10 shows the result obtained for the numerical optimization in relation to the experimental one. At each iteration, the calculation of the coefficient of friction, alteration of the mesh, and the difference between the experimental and the numerical was minimized.

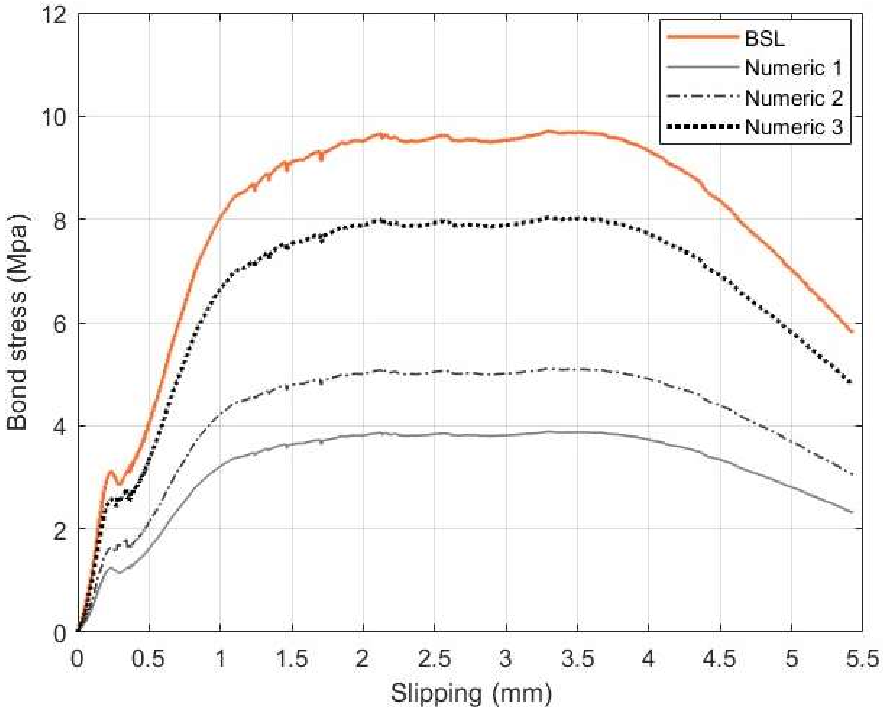


Figure 10. Mesh model. (Own authorship, 2023)

The sample had a maximum deformation of 9.92MPa and a slip of 3.57mm, while its final deformation was 5.87MPa, for the experimental pullout test. It is possible to verify the evolution of the numerical curves, applying the deep learning optimization method. For numerical curve 3, it was possible to find a maximum strain of 8.01MPa and a slip of 3.57mm, while its final strain was 4.81MPa.

## 3. CONCLUSIONS

Based on an experimental pullout test sample, this study focused on optimizing a finite element solution using an inverse method based on deep learning. For this, the simulation was developed in ANSYS APDL ® (2023), which was called in the routine of the MATLAB ® software (2023), which in turn compares the simulation results and from the tolerance arbitrated by the authors, the MATLAB ® software (2023) returns with the convergence response or assigns new parameters for simulations.

It was possible to prove the efficiency of the method applied to approximate the numerical solutions with the experimental solutions. The work is in progress and presents the possibility of improving the contact problem and mesh refinement to enhance the results with greater precision. The optimization demonstrates positive results and sharpens possible advances in other areas of engineering.

For future research, it is recommended to use samples with different contact surfaces, considering that in the experimental data, the influence of the rib between the ribbed and semi-smooth bars eminently influenced the final result. It can also be regarded as refinement in the mesh model or different cases of optimization from the inverse problem since the deep learning method was successful.

## 4. ACKNOWLEDGEMENTS

The first author, Luana C. Bertoncello, is grateful for the financial support of the Coordination for the Improvement of Higher Education Personnel (CAPES - Brazil) in the form of a master's scholarship.

## 5. REFERENCES

ALMEIDA FILHO, F. M. d. Contribuição ao estudo da aderência entre barras de aço e concretos auto-adensáveis. 310 p. Tese (Doutorado) — Universidade de São Paulo, São Carlos, 2006. Citado 18 vezes nas páginas 31, 36, 40, 42, 54, 55, 62, 63, 82, 87, 88, 93, 94, 95, 99, 100, 117 e 131.

ANSYS ®, 2023. “Mechanical APDL Product Launcher 2023 R1”. ANSYS Inc

ANSYS. **PLANE182**: 2-d 4-node structural solid. 2-D 4-Node Structural Solid. Disponível em: https://www.mm.bme.hu/~gyebro/files/ans_help_v182/ans_elem/Hlp_E_PLANE182.html#as7Oxq33mcm. Acesso em: 07 jul. 2023.

CHOI, O. “Effect of rib geometry on bond behavior and failure modes”. In: 8th International Conference on Fracture Mechanics of Concrete and Concrete Structures, FraMCoS, 517– 524p, 2013.

HAYKIN, Simon. **Neural Networks and Learning Machines**. 3. ed. Canadá: Pearson, 2008.

HONG, S.; PARK, S.-K. Uniaxial bond stress-slip relationship of reinforcing bars in concrete. Advances in Materials Science and Engineering, Hindawi, v. 2012, 2012. Citado 3 vezes nas páginas 31, 62 e 69.

KAYABEKIR, A.E., NIGDELI, S.M., BEKDAŞ, G. (2023). The Development of Hybrid Metaheuristics in Structural Engineering. In: Bekdaş, G., Nigdeli, S.M. (eds) Hybrid Metaheuristics in Structural Engineering. Studies in Systems, Decision and Control, vol 480. Springer, Cham.

KLEINERMANN, Jean-Pascal; PONTHOT, Jean-Philippe. Parameter identification and shape/process optimization in metal forming simulation. **Journal Of Materials Processing Technology**, [S.L.], v. 139, n. 1-3, p. 521-526, ago. 2003. Elsevier BV. http://dx.doi.org/10.1016/s0924-0136(03)00530-2.

LUVISON, Jaqueline Maria Borsatti *et al*. Study of the influence of the surface characteristics of steel bars on the steel-concrete interaction. **Brazilian Journal Of Development.** , Curitiba, p. 75145-75163. nov. 2022.

LORRAIN, M. S. et al. “Bond strength and rib geometry: a comparative study of the influence of deformation patterns on anchorage bond strength”. In: PCI Annual Convention & 3rd International FIB Congress FIB, Washington DC, 2010.

MATLAB ®, 2021. “v. R2021a. the language of technical computing”. Mathworks Inc

NARANJO-PÉREZ, Javier; INFANTES, María; JIMÉNEZ-ALONSO, Javier Fernando; SÁEZ, Andrés. A collaborative machine learning-optimization algorithm to improve the finite element model updating of civil engineering structures. **Engineering Structures**, [S.L.], v. 225, p. 111327, dez. 2020. Elsevier BV. http://dx.doi.org/10.1016/j.engstruct.2020.111327.

ROSALES, Y. M. Análise numérico-experimental do comportamento da aderência aço-concreto. 140 p. Dissertação (Mestrado) — Universidade de Brasília, Brasília, 2016. Citado 10 vezes nas páginas 31, 42, 45, 49, 54, 55, 82, 98, 113 e 131.

RUS, G.; GALLEGO, R.; Optimization algorithms for identification inverse problems with the boundary element method. Engineering Analysis with Boundary Elements, v. 26, p. 315-327, 2002.

SIMPLÍCIO, M. A. d. S. Estudo sobre a aderência entre barras de aço e concreto re-forçado com fibras. 263 p. Tese (Doutorado) — Universidade Federal de Pernambuco, Recife, 2008. Citado 6 vezes nas páginas 35, 48, 62, 64, 65 e 66.

STAHLSCHMIDT, J. Estudo de identificação de parâmetros elasto-plásticos utilizando métodos de otimização. 99 f. Dissertação (Mestrado em Ciência e Engenharia de Materiais) — Universidade do Estado de Santa Catarina, Joinville, 2010.

TOJAL, T. L. et al. Contribuição ao estudo da aderência de barras de aço em concreto autoadensável reforçado com fibras metálicas. Dissertação (Mestrado) — Universidade Federal de Alagoas, Maceió, 2011. Citado 2 vezes nas páginas 60 e 98.

## 6. RESPONSIBILITY NOTICE

The author(s) are the only responsible for the printed material included in this paper.